Proceedings of the World Congress on Engineering 2015 Vol I
WCE 2015, July 1 - 3, 2015, London, U.K.

Hermite Collocation and SSPRK Schemes for the Numerical Treatment of a Generalized Kolmogorov-Petrovskii-Piskunov Equation

I.E. Athanasakis , E.P. Papadopoulou and Y.G. Saridakis

Abstract—**In this study we develop high order numerical methods to capture the spatiotemporal dynamics of a generalized Kolmogorov-Petrovskii-Piskunov (KPP) equation characterized by density dependent non-linear diffusion. Towards this direction we consider third order Strong Stability Preserving Runge-Kutta (SSPRK) temporal discretization schemes coupled with the fourth order Hermite cubic Collocation (HC) spatial discretization method. We numerically investigate their convergence properties to reveal efficient HC-RK pairs for the numerical treatment of the generalized KPP equation. The Hadamard product is used to characterize the collocation discretized non-linear equation terms. Several numerical experiments are included to demonstrate the performance of the methods.**

Index Terms—**Generalized Kolmogorov-Petrovskii-Piskunov Equation, Hermite Collocation, Strong Stability Preserving Runge-Kutta, Hadamard product.**

I. Introduction

To incorporate density-dependent active motility to, for instance, biological migration models, described by the Fisher ([1]) or the KPP ([2]) classical equations, is by considering a density-dependent diffusion coefficient $D(u)$ (cf. [3], [4], [5] and the references therein). Assuming that $D(u)$ depends linearly in u, that is $D(u) = \lambda_0 u + \lambda_1$ (cf. [6]), the generalized KPP equation we consider here takes the form:

$$u_t = \mathcal{L}[u] := [(\lambda_1 u + \lambda_0)u_x]_x + \sum_{k=1}^{M} \lambda_{k+1} u^k \ , \qquad (1)$$

where $u \equiv u(x,t)$ and $\lambda_i \in \mathbf{R}$, for all $i = 0, \ldots, M$. For the corresponding Cauchy problem we also assume an initial density distribution $u(x,0) = f(x)$, while for its numerical treatment we also impose Neumann boundary conditions

$$u_x(a,t) = 0 \ \text{ and } \ u_x(b,t) = 0 \qquad (2)$$

away enough form the wave front.

We point out that, the classical KPP problem has been extensively investigated in the literature (see for example [7] - [14] and the references therein) as its contribution to model development in mathematical biology, chemistry, genetics and many, many more important scientific areas, is fundamental.

Manuscript received March 10, 2015; revised April 6, 2015.

This work was supported by the ESF and Greek national funds through the operational program *Education and Lifelong Learning* of the National Strategic Reference Framework (NSRF) THALES (Grant number: MIS-379416).

All authors are with the Applied Math & Computers Lab, Technical University of Crete, 73100 Chania, Crete, Greece

Email of the corresponding author : y.saridakis@amcl.tuc.gr

Aiming at the development of high order numerical schemes for the investigation of the spatiotemporal dynamics of the generalized KPP equation (1), and encouraged of our earlier results presented in [15] for the generalized Fisher equation, in Section 2 we adapt the Hermite Collocation (HC) method, a fourth order scheme, to discretize in space. In Section 3, explicit (to avoid solving nonlinear systems) third order Strong Stability Preserving (SSP) Runge-Kutta time discretization schemes are coupled with the HC method. Their efficiency and convergence properties are numerically investigated in Section 4.

II. Hermite Collocation (HC) Spatial Discretization Method

Assuming sufficiently smooth solutions of equation (1), a uniform partition of $[a,b]$ into N subintervals, with spacing $h = (b-a)/N$ and nodes $x_j := a + jh \ , \ j = 1, \ldots, N+1$, the Hermite Collocation method seeks $O(h^4)$ approximations in the form:

$$U(x,t) = \sum_{j=1}^{N+1} [\alpha_{2j-1}(t)\phi_{2j-1}(x) + \alpha_{2j}(t)\phi_{2j}(x)] \qquad (3)$$

where $\phi_{2j-1}(x)$ and $\phi_{2j}(x)$ are the Hermite cubic nodal basis functions centered over node x_j, described by

$$\phi_{2j-1}(x) = \begin{cases} \phi\left(\frac{x_j - x}{h}\right) & , \quad x \in I_{j-1} \\ \phi\left(\frac{x - x_j}{h}\right) & , \quad x \in I_j \\ 0 & , \quad \text{otherwise} \end{cases} ,$$
$$\phi_{2j}(x) = \begin{cases} -h\psi\left(\frac{x_j - x}{h}\right) & , \quad x \in I_{j-1} \\ h\psi\left(\frac{x - x_j}{h}\right) & , \quad x \in I_j \\ 0 & , \quad \text{otherwise} \end{cases} \qquad (4)$$

with $\phi(s) = (1-s)^2(1+2s) \quad , \quad \psi(s) = s(1-s)^2$ for $s \in [0,1]$.

Equations (3) and (4) directly imply that each Hermite basis function (except the boundary ones) is supported only over two consecutive elements. Hence, over each element $I_j = [x_j, x_{j+1}] \ , \ j = 1, \ldots, N$, there are only 4 non-zero basis functions, and therefore I_j is an element of 4 degrees of freedom (d.o.f.). As an immediate consequence, for $\bar{x} \in I_j$, we may write

$$U(\bar{x},t) = \sum_{\ell=2j-1}^{2j+2} \alpha_\ell(t)\phi_\ell(\bar{x})$$

ISBN: 978-988-19253-4-3
ISSN: 2078-0958 (Print); ISSN: 2078-0966 (Online)

which combined with equation (4) yields the well celebrated Hermite interpolation properties described by

$$\alpha_{2j-1}(t) = U(x_{2j-1}, t) \quad , \quad \alpha_{2j}(t) = U_x(x_{2j-1}, t) \ . \tag{5}$$

Substitution of the approximate solution (3) into equations (1) and (2) yields the residuals

$$\mathcal{R}(x,t) \ := \ U_t(x,t) - \mathcal{L}\left[U(x,t)\right] \tag{6}$$
$$\mathcal{B}(x,t) \ := \ U_x(x,t) \ . \tag{7}$$

For the evaluation of the unknown parameters $\alpha_i \equiv \alpha_i(t)$, $i = 1, \ldots, 2(N+1)$ the Collocation method produces a system of ordinary differential equations (ODEs) by forcing the residual $\mathcal{R}(x,t)$ to vanish at $2N$ *interior collocation* points and the boundary residual $\mathcal{B}(x,t)$ at 2 *boundary collocation* points, namely

$$\mathcal{R}(\sigma_i, t) = 0 \quad , \quad i = 1, \ldots, 2N \tag{8}$$
$$\mathcal{B}(a,t) = 0 \ \text{ and } \ \mathcal{B}(b,t) = 0 \ . \tag{9}$$

Collocation at the Gauss points (cf. [16]) adopts the two roots of the Legendre polynomial of degree 2 in each element I_j , $j = 1, \ldots, N$ to produce the needed interior collocation points. Namely, the $2N$ interior Gaussian collocation points for the element I_j , $j = 1, \ldots, N$ are given by

$$\sigma_{2j-1} = x_j + \frac{h}{2}\left(1 - \frac{1}{\sqrt{3}}\right) \text{ and } \sigma_{2j} = x_j + \frac{h}{2}\left(1 + \frac{1}{\sqrt{3}}\right) . \tag{10}$$

Combination, now, of equations (6), (8) and (10) yields the two *elemental* collocation equations in the from

$$U_t(\sigma_i, t) \ = \ \mathcal{L}\left[U(\sigma_i, t)\right] \ , \ i = 2j-1, 2j \tag{11}$$

or, equivalently, by using (5) and expanding,

$$\begin{aligned} \sum_{\ell=2j-1}^{2j+2} \dot{\alpha}_\ell(t)\phi_\ell(\sigma_i) \ &= \ \left(\lambda_0 + \lambda_1 \sum_{\ell=2j-1}^{2j+2} \alpha_\ell(t)\phi_\ell(\sigma_i)\right) \\ &\cdot \ \sum_{\ell=2j-1}^{2j+2} \alpha_\ell(t)\phi''_\ell(\sigma_i) \\ &+ \ \lambda_1 \left(\sum_{\ell=2j-1}^{2j+2} \alpha_\ell(t)\phi'_\ell(\sigma_i)\right)^2 \\ &+ \ \sum_{k=1}^{M} \lambda_{k+1} \left(\sum_{\ell=2j-1}^{2j+2} \alpha_\ell(t)\phi_\ell(\sigma_i)\right)^k \end{aligned} \tag{12}$$

where, of course, $\dot{\alpha}_\ell(t) = \dfrac{d}{dt}\alpha_\ell(t)$ and $\phi'_\ell(x) = \dfrac{d}{dx}\phi_\ell(x)$.

To express, now, the above elemental equations (12) in matrix form, and avoid lengthy algebraic manipulations, let us first observe that

$$\sum_{\ell=2j-1}^{2j+2} \alpha_\ell(t)\phi_\ell^{(m)}(\sigma_i)\,|_{i=2j-1,2j} = C_j^{(m)}\boldsymbol{\alpha}_j \ , \tag{13}$$

where

$$C_j^{(m)} = \begin{bmatrix} A_j^{(m)} & B_j^{(m)} \end{bmatrix} \ , \ m = 0, 1, 2 \tag{14}$$

$$\boldsymbol{\alpha}_j = \begin{bmatrix} \alpha_{2j-1}(t) & \alpha_{2j}(t) & \alpha_{2j+1}(t) & \alpha_{2j+2}(t) \end{bmatrix}^{\mathrm{T}} \tag{15}$$

with

$$A_j^{(m)} = \begin{bmatrix} \phi_{2j-1}^{(m)}(\sigma_{2j-1}) & \phi_{2j}^{(m)}(\sigma_{2j-1}) \\ \phi_{2j-1}^{(m)}(\sigma_{2j}) & \phi_{2j}^{(m)}(\sigma_{2j}) \end{bmatrix}$$

$$= \frac{1}{h^m}\begin{cases} \begin{bmatrix} s_1^{(m)} & hs_2^{(m)} \\ s_3^{(m)} & -hs_4^{(m)} \end{bmatrix} , & m = 0, 2 \\ \begin{bmatrix} s_1^{(m)} & hs_2^{(m)} \\ s_1^{(m)} & hs_4^{(m)} \end{bmatrix} , & m = 1 \end{cases} \tag{16}$$

$$B_j^{(m)} = \begin{bmatrix} \phi_{2j+1}^{(m)}(\sigma_{2j-1}) & \phi_{2j+2}^{(m)}(\sigma_{2j-1}) \\ \phi_{2j+1}^{(m)}(\sigma_{2j}) & \phi_{2j+2}^{(m)}(\sigma_{2j}) \end{bmatrix}$$

$$= \frac{1}{h^m}\begin{cases} \begin{bmatrix} s_3^{(m)} & hs_4^{(m)} \\ s_1^{(m)} & -hs_2^{(m)} \end{bmatrix} , & m = 0, 2 \\ \begin{bmatrix} s_3^{(m)} & hs_4^{(m)} \\ s_3^{(m)} & hs_2^{(m)} \end{bmatrix} , & m = 1 \end{cases} \tag{17}$$

and

	$m=0$	$m=1$	$m=2$
$s_1^{(m)}$	$\frac{9+4\sqrt{3}}{18}$	-1	$-2\sqrt{3}$
$s_2^{(m)}$	$\frac{3+\sqrt{3}}{36}$	$\frac{\sqrt{3}}{6}$	$-1-\sqrt{3}$
$s_3^{(m)}$	$\frac{9-4\sqrt{3}}{18}$	1	$2\sqrt{3}$
$s_4^{(m)}$	$-\frac{3-\sqrt{3}}{36}$	$-\frac{\sqrt{3}}{6}$	$-1+\sqrt{3}$

.

Using, now, the symbol $\circ$ to denote the Hadamard matrix product, it may easily verified, after some algebraic manipulations, that the matrix form of the elemental equations in (12) may be written as

$$\begin{aligned} C_j^{(0)}\dot{\boldsymbol{\alpha}}_j \ &= \ \lambda_0 C_j^{(2)}\boldsymbol{\alpha}_j + \lambda_1\left(C_j^{(0)}\boldsymbol{\alpha}_j\right)\circ\left(C_j^{(2)}\boldsymbol{\alpha}_j\right) \\ &+ \ \lambda_1\left(C_j^{(1)}\boldsymbol{\alpha}_j\right)\circ\left(C_j^{(1)}\boldsymbol{\alpha}_j\right) \\ &+ \ \sum_{k=1}^{M}\lambda_{k+1}\left(C_j^{(0)}\boldsymbol{\alpha}_j\right)^{\circ k} \ . \end{aligned} \tag{18}$$

Moreover, recall the relations in (5) and observe that

$$\alpha_2(t) = U_x(x_1, t) \equiv U_x(a, t)$$

and

$$\alpha_{2N+2}(t) = U_x(x_{N+1}, t) \equiv U_x(b, t) \ ,$$

which, combined with the boundary residual equations in (7) and (9), yield

$$\alpha_2(t) = \alpha_{2N+2}(t) = 0 \ , \tag{19}$$

hence, also,

$$\dot{\alpha}_2(t) = \dot{\alpha}_{2N+2}(t) = 0 \ . \tag{20}$$

A careful assembly of all elemental and boundary collocation equations, described above, leads to the non-linear

ISBN: 978-988-19253-4-3
ISSN: 2078-0958 (Print); ISSN: 2078-0966 (Online)

Collocation system of ODEs, described by

$$\begin{aligned} C_0\dot{\boldsymbol{\alpha}} &= \lambda_0 C_2\boldsymbol{\alpha} \\ &+ \lambda_1 \left(C_1\boldsymbol{\alpha} \circ C_1\boldsymbol{\alpha} + C_0\boldsymbol{\alpha} \circ C_2\boldsymbol{\alpha}\right) \\ &+ \sum_{k=1}^{M} \lambda_{k+1} \left(C_0\boldsymbol{\alpha}\right)^{\circ k} \end{aligned} \tag{21}$$

where the $2N \times 2N$ matrices $C_m,\ m = 0, 1, 2$ are described by

$$C_m = \begin{bmatrix} \tilde{A}_1^{(m)} & B_1^{(m)} & & & & \\ & A_2^{(m)} & B_2^{(m)} & & & \\ & & \ddots & \ddots & & \\ & & & A_{N-1}^{(m)} & B_{N-1}^{(m)} & \\ & & & & A_N^{(m)} & \tilde{B}_N^{(m)} \end{bmatrix}$$

while the $2N \times 1$ vectors $\boldsymbol{\alpha} \equiv \boldsymbol{\alpha}(t)$ and $\dot{\boldsymbol{\alpha}} \equiv \dot{\boldsymbol{\alpha}}(t)$ are described by

$$\boldsymbol{\alpha} = \begin{bmatrix} \alpha_1(t) & \alpha_3(t) & \alpha_4(t) & \cdots & \alpha_{2N}(t) & \alpha_{2N+1}(t) \end{bmatrix}^{\mathrm{T}}$$
$$\dot{\boldsymbol{\alpha}} = \begin{bmatrix} \dot{\alpha}_1(t) & \dot{\alpha}_3(t) & \dot{\alpha}_4(t) & \cdots & \dot{\alpha}_{2N}(t) & \dot{\alpha}_{2N+1}(t) \end{bmatrix}^{\mathrm{T}}.$$

The 2×2 matrices $\tilde{A}_1^{(k)}$ and $\tilde{B}_N^{(k)}$ are obtained by omitting the second column of the matrices $A_1^{(k)}$ and $B_N^{(k)}$ respectively, as the vanishing parameters α_2 and α_{2N+2} have been omitted.

Concluding this section we point out that the linear independence of the Hermite cubic basic functions yields the non-singularity of the coefficient matrix C_0 of the Collocation ODE system in (21) implying the unique solution of the system for any fixed $t = t_n$ and the existence, of course, of the inverse C_0^{-1}.

III. Strong Stability Preserving Runge-Kutta Time Discretization Schemes

High order strong stability preserving (SSP) Runge-Kutta methods were developed (cf. [17], [18], [19]) for the time discretization of the semi-discrete system obtained from the spatial discretization of PDEs by a finite difference or finite element method.

The SSPRK methods were originally developed for the solution of the semi-discrete ODE system

$$\boldsymbol{v}_t = F(\boldsymbol{v}) \quad ,$$

arising from the hyperbolic equation

$$v_t + f(v)_x = 0 \quad ,$$

and aimed to the preservation of the Total Variation Diminishing (TVD) property satisfied by an appropriately chosen spatial discretization coupled with forward Euler (FE) integration. The essence of the SSPRK time discretization methods lies on their ability to maintain strong stability while increasing the order of accuracy, under the hypothesis that forward Euler is strongly stable and providing suitable restrictions of the time stepping. Namely, assuming that, for any given norm, semi-norm or convex functional $||\cdot||$, the FE satisfies the strong stability requirement

$$||\boldsymbol{v}_{FE}^n + \Delta t F(\boldsymbol{v}_{FE}^n)|| \leq ||\boldsymbol{v}_{FE}^n|| \ ,$$

with $\boldsymbol{v}_{FE}^n := \boldsymbol{v}_{FE}(t_n)$ and $t_n := n\Delta t$, $n = 1, 2 \ldots$ for sufficiently small $\Delta t \leq \Delta t_{FE}$, the SSP discretization satisfies

$$||\boldsymbol{v}^{n+1}|| \leq ||\boldsymbol{v}^n|| \ \text{ for } \ \Delta t \leq c\Delta t_{FE} \ .$$

Adapting the SSPRK class of time discretization methods for the solution of parabolic problems is not always efficient. The stiffness of the some parabolic operators, even when the hyperbolic part dominates, may affect the stability region hence, also, the effectiveness of the methods. However, the simplicity, the effectiveness and the explicit nature of the SSP class of methods should not be over passed with ease, especially for parabolic operators with mild stiffness problems.

In this work, for the solution the semi-discrete non-linear Collocation system of ODEs in (21), which is rewritten for the needs of this section as

$$\dot{\boldsymbol{\alpha}} = C(\boldsymbol{\alpha}) \tag{22}$$

where, of course,

$$\begin{aligned} C(\boldsymbol{\alpha}) &:= \lambda_0 C_0^{-1} C_2\boldsymbol{\alpha} \\ &+ \lambda_1 C_0^{-1} \left(C_1\boldsymbol{\alpha} \circ C_1\boldsymbol{\alpha} + C_0\boldsymbol{\alpha} \circ C_2\boldsymbol{\alpha}\right) \\ &+ \sum_{k=1}^{M} \lambda_{k+1} C_0^{-1} \left(C^{(0)}\boldsymbol{\alpha}\right)^{\circ k} \quad , \end{aligned} \tag{23}$$

we consider two optimal (cf. [20], [21]) third order stage three and stage four SSP schemes, which are denoted by SSP(3,3) and SSP(4,3) and they are written in the form:

$$\underline{SSP(3,3)}$$

$$\begin{aligned} \boldsymbol{\alpha}^{(1)} &= \boldsymbol{\alpha}^n + \Delta t C(\boldsymbol{\alpha}^n) \\ \boldsymbol{\alpha}^{(2)} &= \tfrac{3}{4}\boldsymbol{\alpha}^n + \tfrac{1}{4}\boldsymbol{\alpha}^{(1)} + \tfrac{1}{4}\Delta t C(\boldsymbol{\alpha}^{(1)}) \\ \boldsymbol{\alpha}^{n+1} &= \tfrac{1}{3}\boldsymbol{\alpha}^n + \tfrac{2}{3}\boldsymbol{\alpha}^{(2)} + \tfrac{2}{3}\Delta t C(\boldsymbol{\alpha}^{(2)}) \end{aligned}$$

and

$$\underline{SSP(4,3)}$$

$$\begin{aligned} \boldsymbol{\alpha}^{(1)} &= \boldsymbol{\alpha}^n + \tfrac{1}{2}\Delta t C(\boldsymbol{\alpha}^n) \\ \boldsymbol{\alpha}^{(2)} &= \boldsymbol{\alpha}^{(1)} + \tfrac{1}{2}\Delta t C(\boldsymbol{\alpha}^{(1)}) \\ \boldsymbol{\alpha}^{(3)} &= \tfrac{2}{3}\boldsymbol{\alpha}^n + \tfrac{1}{3}\boldsymbol{\alpha}^{(2)} + \tfrac{1}{6}\Delta t C(\boldsymbol{\alpha}^{(2)}) \\ \boldsymbol{\alpha}^{n+1} &= \boldsymbol{\alpha}^{(3)} + \tfrac{1}{2}\Delta t C(\boldsymbol{\alpha}^{(3)}) \end{aligned}$$

Once the initial vector $\boldsymbol{\alpha}^0$ has been determined, we can compute the solutions at the required time steps of the above equations. The initial vector $\boldsymbol{\alpha}^0$ can be easily determined by making use of the basic Hermite interpolation properties, described in (5), and the initial condition $u(x, 0) = f(x)$. In

ISBN: 978-988-19253-4-3
ISSN: 2078-0958 (Print); ISSN: 2078-0966 (Online)

doing so one may obtain

$$\boldsymbol{\alpha}^0 = \begin{bmatrix} \alpha_1(0) \\ \alpha_3(0) \\ \alpha_4(0) \\ \vdots \\ \alpha_{2N-1}(0) \\ \alpha_{2N}(0) \\ \alpha_{2N+1}(0) \end{bmatrix} = \begin{bmatrix} U(x_1,0) \\ U(x_2,0) \\ U_x(x_2,0) \\ \vdots \\ U(x_{N-1},0) \\ U_x(x_{N-1},0) \\ U(x_N,0) \end{bmatrix} = \begin{bmatrix} f(x_1) \\ f(x_2) \\ f'(x_2) \\ \vdots \\ f(x_{N-1}) \\ f'(x_{N-1}) \\ f(x_N) \end{bmatrix} \tag{24}$$

IV. Numerical Results

Several different model problems are used in this section for the assessment of the HC-SSPRK schemes. The spatial absolute error

$$\mathcal{E}_n := ||U(x,t_n) - u(x,t_n)||_2$$

is used in all experiments to measure the accuracy of the numerical approximations in each time step $t = t_n$, while their infinity norm over all time steps

$$\mathcal{E}_\infty = \max_n \{\mathcal{E}_n\}$$

is adapted to evaluate the overall accuracy of the numerical space-time integration. The order of convergence (O.o.C) of the Collocation method, as well as the computational time needed to reach time level $t = 2$, are also used to demonstrate the preservation of the expected accuracy and the efficiency of the methods.

Model Problem I

The first model problem, used to investigate the performance of the HC-RK methods, is described by

$$u_t = [(1-2u)u_x]_x + \frac{1}{2}u - u^2$$
$$u_x(-\pi,t) = 0, \quad u_x(\pi,t) = 0$$
$$u(x,0) = \frac{1}{2} - \frac{1}{6}\left(1 + \sin\frac{x}{2}\right)$$

and admits the exact solution (cf. [6])

$$u(x,t) = \frac{1}{2} - \frac{1}{3}\left(1 + \sin\frac{x}{2}\right)\left(1 + e^{\frac{t}{2}}\right)^{-1} .$$

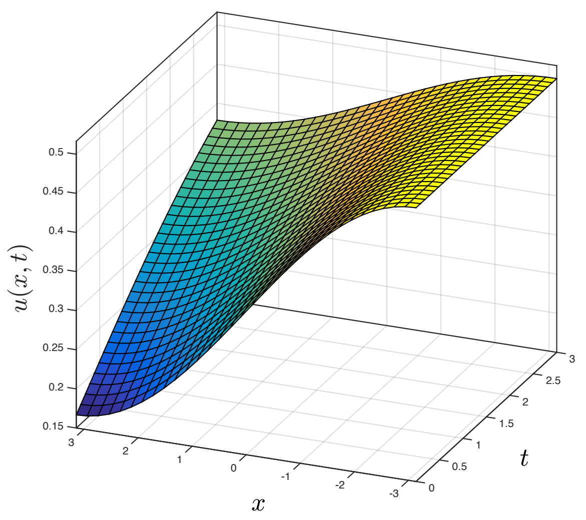

Fig. 1: Plot of the exact/numerical solution

The results obtained from all experiments for this model problem, are reported my means of Table I and Figure 2 that follow.

TABLE I Computational Performance of HC-RK schemes

	Error Norm $\mathcal{E}_\infty$	*Collocation's O.o.C.*	*Time (sec) needed to reach* $t = 2$	
h	SSP(4,3)/(3,3)	SSP(4,3)/(3,3)	SSP(4,3)	SSP(3,3)
1/4	2.91e-07	-	0.07	0.21
1/8	1.97e-08	3.88	0.26	0.76
1/16	1.28e-09	3.94	1.19	3.37
1/32	8.01e-11	3.99	5.22	15.74
1/64	5.05e-12	3.98	28.38	88.38

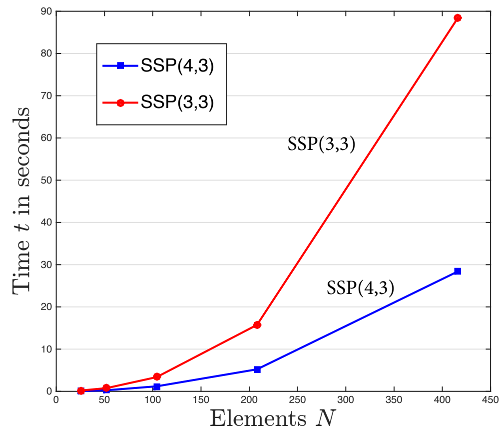

Fig. 2: Time comparison in seconds between SSPRK(4,3)-(3,3) and RK4.

The CFL conditions, imposed on time stepping, are numerically found to satisfy

$$\Delta t \leq \frac{1}{5}h^2 \quad \text{for SSPRK(4,3)}$$
$$\Delta t \leq \frac{1}{10}h^2 \quad \text{for SSPRK(3,3)}$$

and, apparently, favor the SSPRK(4,3) scheme. Under these restrictions both time discretization schemes remain strongly stable, as it is depicted in Figure 3 for SSPRK(4,3), and at

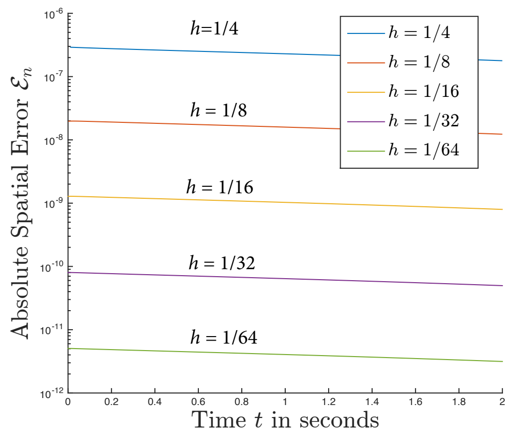

Fig. 3: Spatial absolute error as a function of time for the HC-SSPRK(4,3)

the same time, produce identical high accuracy error results while preserving the $O(h^4)$ order of convergence of the HC method (see Table I). However, due to the CFL condition, the SSPRK(4,3) outperforms HC-SSRK(3,3) (see Table I and Figure 2) method despite the fact that it needs the calculation of an extra stage.

Model Problem II

The second model problem, used to investigate the performance of the HC-RK methods, is described by

$$u_t = \frac{1}{100}u_{xx} + \frac{1}{4}u\left(1-u^3\right)$$
$$u_x(-10,t)=0, \quad u_x(5,t)=0$$
$$u(x,0) = 1 + (2^{3/2}-1)e^{(-15\sigma_1 x)^{-2/3}}$$

and admits the exact solution (cf. [11])

$$u(x,t) = 1 + (2^{3/2}-1)e^{(-\frac{3}{2}\sigma_1(10x+2\lambda_1 t))^{-2/3}}$$

where $\sigma_1 = \lambda - \sqrt{\lambda^2 - \frac{1}{4}}$ and $\lambda = \frac{7\sqrt{2}}{16\sqrt{5}}$.

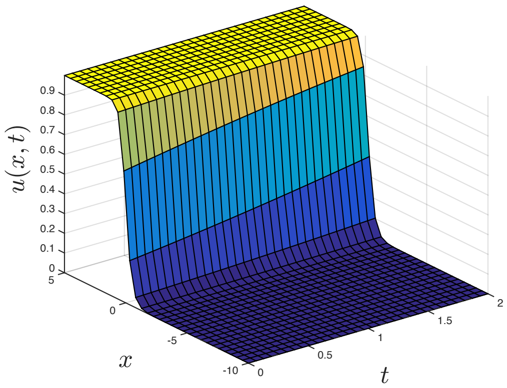

Fig. 4: Plot of the exact/numerical solution

The results obtained from all experiments for this model problem, are reported my means of Table II and Figure 5 that follow.

TABLE II Computational Performance of HC-RK schemes

	Error Norm $\mathcal{E}_\infty$	Collocation's O.o.C.	Time (sec) needed to reach $t=2$	
h	SSP(4,3)/(3,3)	SSP(4,3)/(3,3)	SSP(4,3)	SSP(3,3)
1/4	2.17e-04	-	0.10	0.17
1/8	1.42e-05	3.93	0.51	0.83
1/16	8.84e-07	4.00	2.85	4.57
1/32	5.52e-08	4.00	18.60	29.48
1/64	3.45e-09	4.00	134.71	208.29

The CFL conditions, imposed on time stepping, are numerically found to satisfy

$$\Delta t \le \frac{1}{8}\,h^2 \quad \text{for SSPRK(4,3)}$$
$$\Delta t \le \frac{1}{16}h^2 \quad \text{for SSPRK(3,3)}$$

and, apparently, favor the SSPRK(4,3) scheme. Under these restrictions both time discretization schemes remain stable, as it is depicted in Figure 6 for SSPRK(4,3), and at the same time, produce identical high accuracy error results while preserving the $O(h^4)$ order of convergence of the HC method (see Table II). However, due to the CFL condition, the SSPRK(4,3) outperforms HC-SSRK(3,3) (see Table II and Figure 5) method despite the fact that it needs the calculation of an extra stage.

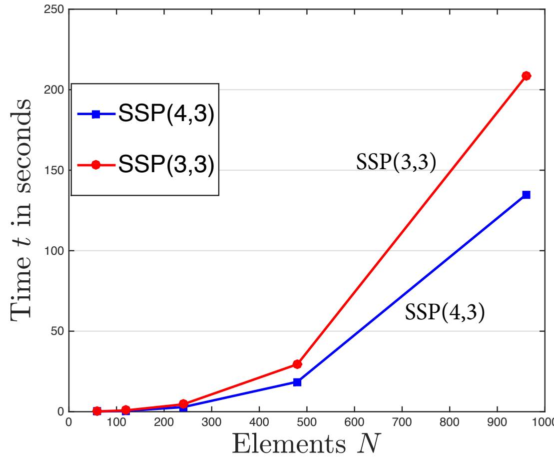

Fig. 5: Time comparison in seconds between SSPRK(4,3)-(3,3) and RK4.

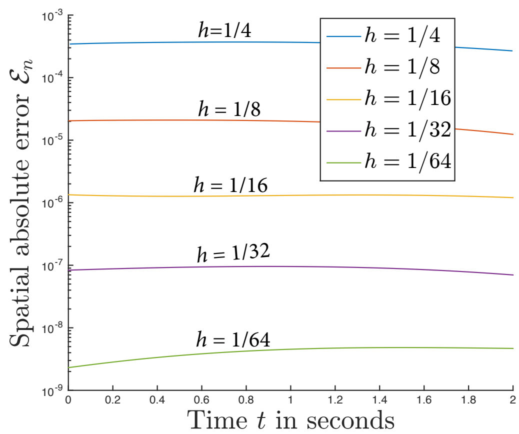

Fig. 6: Spatial absolute error as a function of time for the HC-SSPRK(4,3)

Model Problem III

The third model problem, used to investigate the performance of the HC-RK methods, is described by

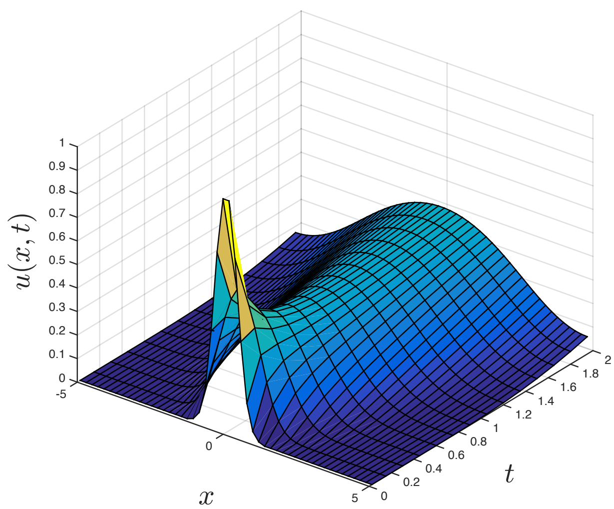

Fig. 7: Plot of the numerical solution

ISBN: 978-988-19253-4-3
ISSN: 2078-0958 (Print); ISSN: 2078-0966 (Online)

$$u_t = \left[\left(\frac{1}{10}u + 1\right) u_x\right]_x + u - u^2 - 2u^3$$
$$u_x(-5,t) = 0, \quad u_x(5,t) = 0$$
$$u(x,0) = \frac{1}{0.4\sqrt{\pi}} e^{-\left(\frac{x}{0.4}\right)^2} .$$

The results obtained from all experiments for this model problem, are reported my means of Table III and Figure 8 that follow.

TABLE III Computational Performance of HC-RK schemes

	Error Norm $\mathcal{E}_\infty$	*Collocation's O.o.C.*	*Time (sec) needed to reach* $t = 2$	
h	SSP(4,3)/(3,3)	SSP(4,3)/(3,3)	SSP(4,3	SSP(3,3)
1/4	1.72e-05	-	0.18	0.27
1/8	1.26e-06	3.77	0.78	1.20
1/16	8.17e-08	3.94	3.93	6.17
1/32	5.15e-09	3.98	23.03	36.14
1/64	3.24e-10	3.98	147.29	252.05

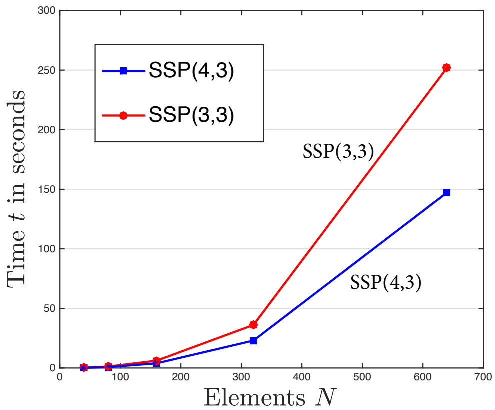

Fig. 8: Time comparison in seconds between SSPRK(4,3)-(3,3) and RK4.

The CFL conditions, imposed on time stepping, are numerically found to satisfy

$$\Delta t \leq \frac{1}{10}\, h^2 \quad \text{for SSPRK(4,3)}$$
$$\Delta t \leq \frac{1}{20} h^2 \quad \text{for SSPRK(3,3)}$$

and favor consistently the SSPRK(4,3) scheme. Under these restrictions both time discretization schemes produce identical high accuracy error results while preserving the $O(h^4)$ order of convergence of the HC method (see Table III). However, due to the CFL condition, the SSPRK(4,3) outperforms HC-SSRK(3,3) (see Table III and Figure 8) method despite the fact that it needs the calculation of an extra stage.

Conclusion

In this work, the fourth order HC is coupled to third order $SSPRK$ schemes for the treatment of a generalized Fisher equation. Numerical results presented, imply that HC-SSPRK(4,3) method is a very competitive, effective and stable space-time integration scheme. For stiff parabolic problems and problems with large derivative variations other type time integration schemes and adaptive grids will be used in future work.

Acknowledgement

The present research work has been co-financed by the European Union (European Social Fund ESF) and Greek national funds through the Operational Program Education and Lifelong Learning of the National Strategic Reference Framework (NSRF) - Research Funding Program: THALES (Grant number: MIS-379416). Investing in knowledge society through the European Social Fund.

References

[1] Fisher RA *The wave of advance of advantageous genes*, Ann. Eugen., **7**, 255-369, 1937

[2] Kolmogorov AN, Petrovskii IG and Piskunov NS *Investigation of the equation of diffusion combined with increasing of the substance and its application to a biology problem*, Bull. Moscow State Univ. Ser. A: Math. and Mech., **1(6)**, 1-25, 1937

[3] Hengeveld R *Dynamics of Biological Invasions*, Chapman and Hall, London, 1989

[4] Murray JD *Mathematical Biology*, Springer, Berlin, 1989

[5] Petrovskii SV and Li BL *Exactly Solvable Models of Biological Invasion*, Taylor & Francis, 2010

[6] Cherniha R and Dutka V *Exact and Numerical Solutions of the Generalized Fisher Equation*, Reports on Mathematical Physics, **47**, 393-412, 2001

[7] Fitzhugh R *Impulses and physiological states in models of nerve membrane*, Biophys. J., Vol. 1(445), 1961

[8] Nagumo JS, Arimoto S and Yoshizawa S *An active pulse transmission line simulating nerve axon*, Proc. IRE, Vol. 50,(2061), 1962

[9] Newell AC and Whitehead JA *Finite bandwidth, finite amplitude convection*, J. Fluid Mech., Vol. 38, 279, 1969

[10] Aronson DG and Weinberger HF, *Nonlinear diffusion in population genetics, combustion and nerve pulse propagation*, In Partial Dierential Equations and Related Topics (Edited by J. A. Goldstein), Lecture Notes in Mathematics, Vol. 446, pp. 5-49. Springer, Berlin, 1975

[11] Kametaka Y *On the nonlinear diffusion equation of Kolmogorov-Petrovskii-Piskunov type*, Osaka J. Math. 13, 11-66, 1976

[12] Ma WX, Fuchssteiner B *Explicit and Exact Solutions to a Kolmogorov-Petrovskii- Piskunov Equation*, Internat. J. Non-Linear Mech. 31 (3), 329-338, 1996

[13] Needham DJ and King AC *The evolution of travelling waves in the weakly hyperbolic generalized Fisher model*, Proc. Roy. Soc. (London), Vol. 458(1055), 2002

[14] Nikitin AG, Barannyk TA *Solitary wave and other solutions for nonlinear heat equations*, CEJM 2(5) 840858, 2005

[15] Athanassakis IE, Papadopoulou EP and Saridakis YG *Runge-Kutta and Hermite Collocation for a biological invasion problem modeled by a generalized Fisher equation*, Proceedings of the IC-MSQUARE 2013 Conference, Prague

[16] de Boor C and Swartz B *Collocation at Gaussian points*, SIAM Num. Anal., vol. 10, pp. 582-606, 1973

[17] Shu CW *Total-variation-diminishing time discretizations*, SIAM J. Sci. Stat. Comput., **9**, 1073-1084, 1988

[18] Shu CW and Osher S *Efficient implementation of essentially non-oscillatory shock-capturing schemes*, J. Comput. Phys., **77**, 439-471, 1988

[19] Gottlieb S, Shu CW and Tadmor E *Strong Stability-Preserving High-Order Time Discretization Methods*, SIAM Num. Anal., **43**, 89-112, 2001

[20] Gottlieb S and Shu CW *Total variation diminishing Runge-Kutta schemes*, Mat. Comp., **67**, 73-85, 1998

[21] Ruuth S and Spiteri R *Two barriers on strong-stability-preserving time discretization methods*, J. Scientific Computation, **17**, 211-220, 2002

[22] Duan WS, Yang HJ and Shi YR *An exact solution of Fisher equation and its stability*, Chinese Physics, **15**, 1414-17, 2006